

Stray Light View of Accreting Atolls: GX 9+9

Lynn Yang

Mentors: Fiona A. Harrison, Renee Ludlam

1 Abstract

Due to the open geometry of the mast on Nuclear Spectroscopic Telescope Array (NuSTAR), we can observe and analyze the light from nearby X-ray sources that fall on the detectors of the telescope, known as stray light. The focus of this project is on the object, GX 9+9, which is an accreting atoll source, determined by the island-shaped region of the source on a hard-intensity diagram (HID). I can utilize the NuSTAR stray light observations of GX 9+9 to enhance our understanding of accretion and the properties of neutron stars (NSs). Observing the location of observations on the HID can determine the spectral state of GX 9+9 over time. The stray light data allows us to model the continuum spectra and reflection emission of the accreting system. The fitted models of the spectra give us the appropriate values to also calculate the radius constraints and the extent of the boundary layer between the accretion disk and the NS surface of GX 9+9.

2 Overview

2.1 Background Information

Neutron stars (NSs) are the densest observable objects with a surface in the universe, and of those objects, low-mass X-ray binaries (LMXB) are of particular interest because of its accretion disk. These specific accretion disks of material form from the Roche-Lobe overflow from their low-mass companion star, similar in size to that of our Sun. There are two types of persistently accreting NS LMXBs known as “Z” and “atoll” sources which are named after the shapes traced out in color-color and hardness-intensity diagrams (HID) [1]. In this project, we will focus on looking at the atoll sources which are typically less luminous [2]. An HID plots the ratio of the X-ray emission in different energy bands versus the total emission from the system to characterize what spectral state the system is in.

The Nuclear Spectroscopic Telescope Array (NuSTAR) is a great mission to observe these X-ray bright persistently accreting systems. The NuSTAR observatory has a 10 meter deployable mast that allows it to focus ‘hard’ X-rays from 3-79 keV onto two focal plane modules (FPMA and FPMB) [3]. Due to the open geometry of the mast, light from nearby bright X-ray sources can fall on the detectors via the open aperture stop. This is known as stray light, which is light that is not focused by the optics [4], and has led to a plethora of serendipitous data sets on these bright accreting NS sources with which to look at these systems in a new way.

2.2 NuSTAR Group

Professor Harrison is the Principal Investigator for NuSTAR and the group works extensively on mission operations and with the data. I am working with Dr. Ludlam who did her PhD work on the properties of accreting NS systems using NuSTAR data. More specifically, I’m working with the Straycats group which deals with data analysis of stray light from NuSTAR observations. We have weekly meetings, or Stray Light Tag-ups, where we discuss our progress and talk about any issues we’ve run into.

2.3 Objective

In this research, I will utilize NuSTAR stray light observations to enhance our understanding of accretion and the properties of NSs. This will require delving into StrayCats¹ for target selection and data reduction to generate HIDs and determine spectral changes. Location on the HID corresponds to spectral state; therefore, we can use these to gauge changes in the overall emission from these systems and infer properties about accretion and the NS. These properties include determining magnetic field strength of the NS, an upper limit on NS radius, and/or detecting boundary layer regions between the accretion disk and NS surface [2].

3 Methods

In summary, a sample of persistent NS LMXBs stray light observations that have a stray light pattern area on one of the detector modules (FPMA or FPMB) that is $\geq 1 \text{ cm}^2$ and an exposure time $\geq 30 \text{ ks}$ have been selected. This data set has over 30 observations that comprises more than 2 megaseconds of data. Data from these observations will be reduced using mission specific software (HEASoft) and tools (nustar-gen-utils²) in “Det1” coordinates. Light-curves are extracted in different energy bands to create the HID which will then be assessed to determine the appropriate points in which spectra will be extracted to determine the different properties of the system in relation to the position on the HID.

I will also lay out the more specific process in which I have been approaching my objective. At first, we used a test observation (obsID 10202005004) to learn how we will work with future data. For the test observation, I went through each Python code through the terminal, but I ended up creating a Python notebook that can run all the code without needing the terminal.

First, I downloaded and set up the softwares that are necessary for this project which include SAOImageDS9, XSPEC, and HEASoft, among others. Before running the commands in the terminal for the data, we need to go into the bash terminal with ‘./bashrc’, activate NuSTAR with ‘source activate nustar’, and initiate HEASoft and the calibration with ‘heainit’ and ‘caldb’ in the terminal. I download the .tar files for observations from lif, and once that is complete, I go to nustarsoc.caltech.edu to look at the background filtering reports. To figure out which filtering report is the best option, I find one that has relatively low variability in cts/sec throughout the duration of the observation that also has a high effective exposure time. I then use the nucalcsaa options from the most effective report to use in nupipeline if necessary. Some do not require any options like nu90601310002 or nu60002032004, for example. I then create an .SLproducts directory for each observation ID.

Once all of that is complete, I now have everything ready to run through the Python notebook. First, I run det1image.py which will create .fits files for both FPMA and FPMB. Then I go to the terminal where I open up the ds9 fits file that I just obtained which will open up the ds9 software, SAOImageDS9. Once the file is open, I create region files for the source and the background. For the source, it’s important to note whether or not the source is included or excluded, and the inclusion must be placed first before the exclusion. Examples of what this step would look like are shown below.

¹<https://nustarstraycats.github.io/straycats/>

²<https://github.com/NuSTAR/nustar-gen-utils>

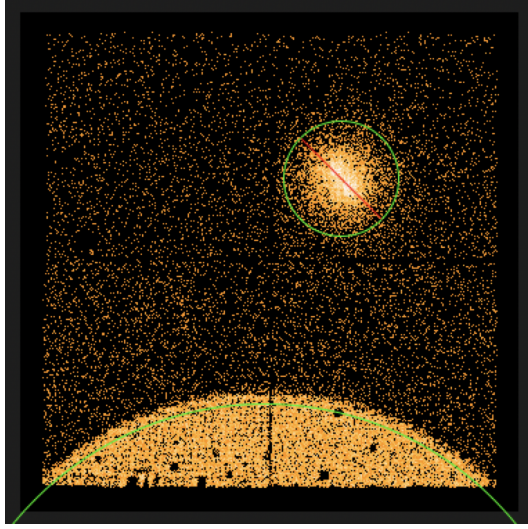


Figure 1: Source image on ds9 for nu60002032002

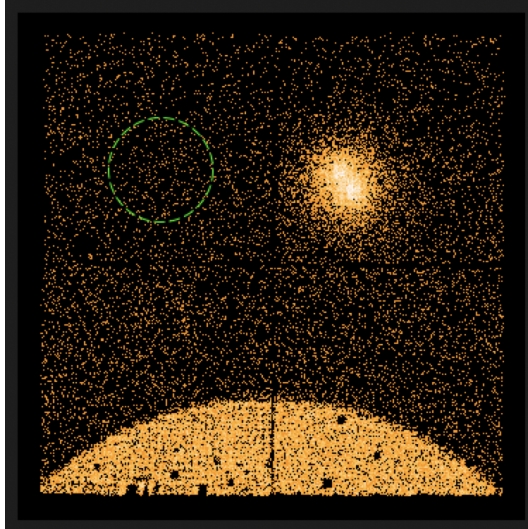


Figure 2: Background image on ds9 for nu60002032002

I save both source and background separately as ds9 files in the image coordinate system. I then run `mkexpomap.py` to create an exposure map then run the exposure map shell script on the terminal. Back on the Python notebook, I extract the light curves and run the three shell scripts on the terminal. Then I create an HID and CCD using `SL_LS_HID.py`. I then run `straylightspec.py` and `bkgstraylightspec.py` and run the shell scripts for the source and background to create the straylight spectrum. Then I create arf files, find the region area, and edit the BACKSCAL region area for the obsIDs. Once all of this is done, I can start using XSPEC to fit models. When using XSPEC, I create another .pha file to regroup the original file; so far, I've used the optimal grouping and bin 3 groups. I also want to make sure the x-axis of the graph is in energy instead of channels, and to ignore any bins that are less than 3 keV because the telescope is best calibrated for energies above 3 keV. The model I will be using to fit the data is a tbabs model with diskbb (disk blackbody) and bbody (blackbody) which I demonstrated with nu60002032002 in the Progress section.

Then I create and fit models on Xspec and tabulate the important parameter values. First, I took the already existing .pha file of the source observation and optimally bin the file. With the optimally binned file, I observed the 3-20 keV range and created a model for the data. For most of the observations, I used the `tbabs*(diskbb+bbody)` model; however, for one of the observations, I utilized the `tbabs*(diskbb+nthComp)` model. Then I fit the model to the data and save the parameter values of the newly fitted model, and I make sure that the fit statistic is in C-statistic. Afterwards, I check for the error ranges for each parameter and the absorbed and unabsorbed fluxes of the observation between 0.5 to 50 keV, and I tabulate the corresponding values. The following are examples of these steps for the observation nu90101008002 in FPMA.

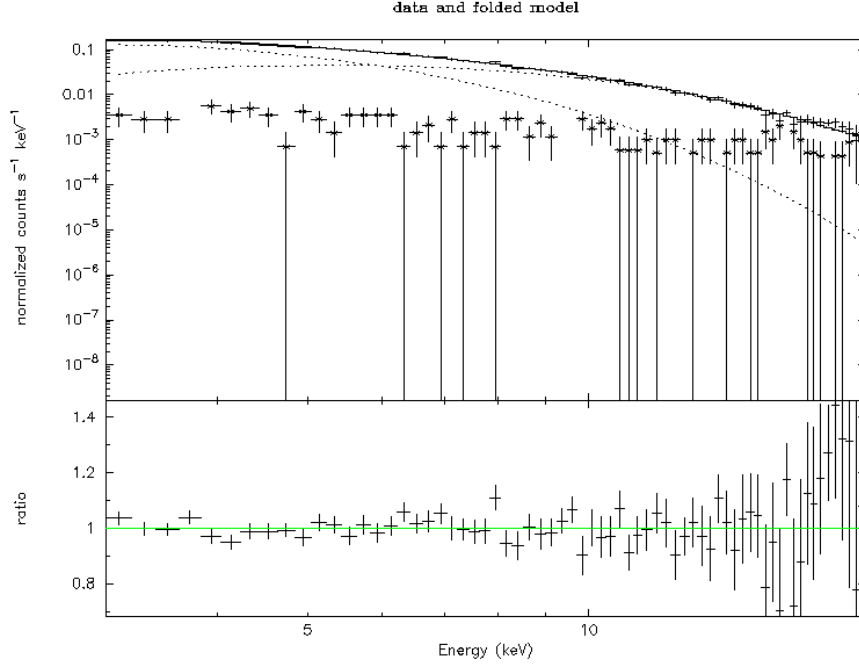


Figure 3: Fitted spectrum with `tbabs*(diskbb+bbody)` of nu90101008002 (FPMA) and ratio of model

```
=====
Model TBabs<1>(diskbb<2> + bbody<3>) Source No.: 1 Active/On
Model Model Component Parameter Unit Value
par comp
1 1 TBabs nH 10^22 0.190000 frozen
2 2 diskbb Tin keV 1.34313 +/- 7.02127E-02
3 2 diskbb norm 81.2732 +/- 15.8585
4 3 bbody kT keV 2.19364 +/- 6.65822E-02
5 3 bbody norm 3.49168E-02 +/- 2.52215E-03
=====

Using energies from responses.

Fit statistic : C-Statistic 54.49 using 68 bins.
Test statistic : Chi-Squared 55.09 using 68 bins.
Null hypothesis probability of 7.79e-01 with 64 degrees of freedom
```

Figure 4: Parameter values of the fitted model for nu90101008002 (FPMA)

I manipulated the code from the Python notebook I used to create HIDs for each individual

observation in order to make a composite HID for all the observations for GX 9+9. I executed this by creating an array of the observations, and the colors I used corresponded to the colors I used in the Swift/BAT and MAXI long-term light curve. In order to better view the HID, I binned all of the observations by 500 seconds.

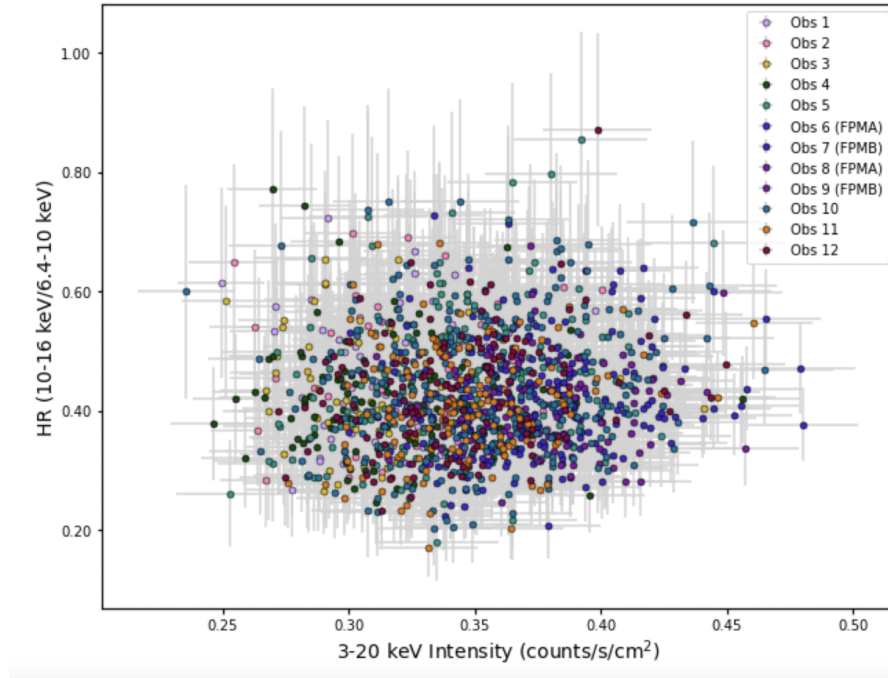


Figure 5: Composite HID with all the GX 9+9 observations

From the values obtained by fitting the stray light data into Xspec, I determined the confidence errors for each value and the absorbed and unabsorbed fluxes for each observation. I then ran Python files that helped me calculate the spherical inner disk radius and banded inner disk radius inferred from the blackbody normalization and the inner disk radius inferred from the disk blackbody normalization. I was able to calculate these values for every observation except for nu60002032002 where I only had values to calculate the inner disk radius calculated from the disk blackbody component. We chose not to also use the comptonized blackbody because according to the 2009 Savolainen paper, they concluded that the Comptonization parameters were found to be unnecessary because there was too little hardening to distort the shape of the blackbody to be detected. In order to determine these values, I also used a color correction factor and assumed that the distance to GX 9+9 was 6 kpc and the inclination was 47 degrees.

4 Results

A summary of the observation, FPM, inner disk radius calculated from the disk blackbody and blackbody components, and luminosities are listed in the table below.

Obs	Sequence ID	FPM	R_{in} (diskbb)	Banded R_{in} (bbody)	Luminosity
1	90101008002	A	18.93 km	18.73 km	$3.53\text{e}+37$ ergs/s
		B	18.29 km	17.43 km	$3.34\text{e}+37$ erg/s
2	60402007002	A	16.04 km	17.53 km	$3.15\text{e}+37$ erg/s
3	60002032008	A	17.91 km	19.58 km	$2.94\text{e}+37$ erg/s
4	60402007004	A	13.45 km	13.60 km	$3.08\text{e}+37$ erg/s
5	60002032004	A	18.40 km	16.84 km	$3.07\text{e}+37$ erg/s
6	90101008004	A	17.93 km	15.41 km	$3.59\text{e}+37$ erg/s
		B	20.04 km	19.07 km	$3.66\text{e}+37$ erg/s
7	60002032006	A	19.55 km	20.14 km	$2.93\text{e}+37$ erg/s
8	60002032002*	A	11.84 km		$2.90\text{e}+37$ erg/s
9	60002032010	B	17.41 km	17.11 km	$3.28\text{e}+37$ erg/s
10	60201020002	B	17.94 km	17.52 km	$3.39\text{e}+37$ erg/s

Figure 6: Summary of the calculated values for each observation

Shown below is also a Swift/BAT and MAXI long-term light curve of all ten observations. We want to mainly focus on the four observations that are close in time with each other on the very left to observe how GX 9+9 may change throughout short time intervals.

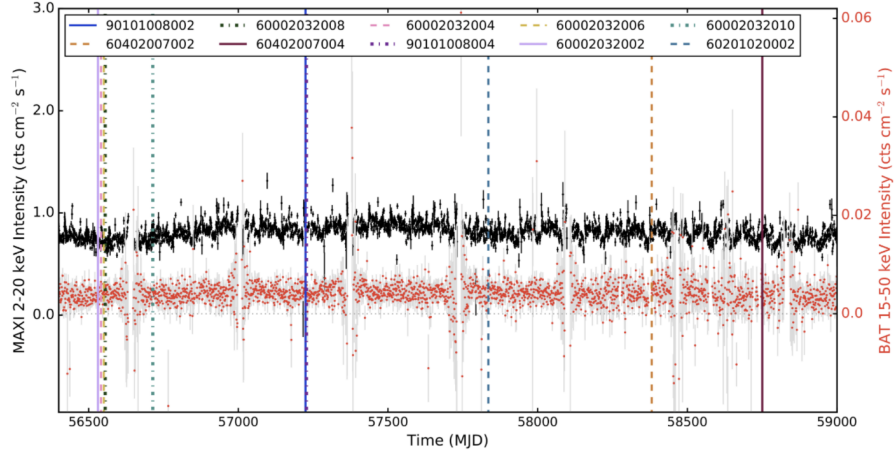


Figure 7: Swift/BAT and MAXI long-term light curve

We can observe the composite HID and highlight the first four observations and compare them to the rest of the observations, which is what I have done in the HID below where the first four are colored and the others are grayed out. From this, we can see that there were minimal differences between the four as they tended to cluster near the left area compared to all of the observations. However, one likely reason why the data points are skewed more towards the left is the lower overall luminosity between the beginning four observations compared to that of the rest of the observations. This corresponds well to Figure 6 where we display the luminosities of all the observations. In Figure 9, I rearranged these four observations to the top to better observe the lower luminosity between these observations in particular.

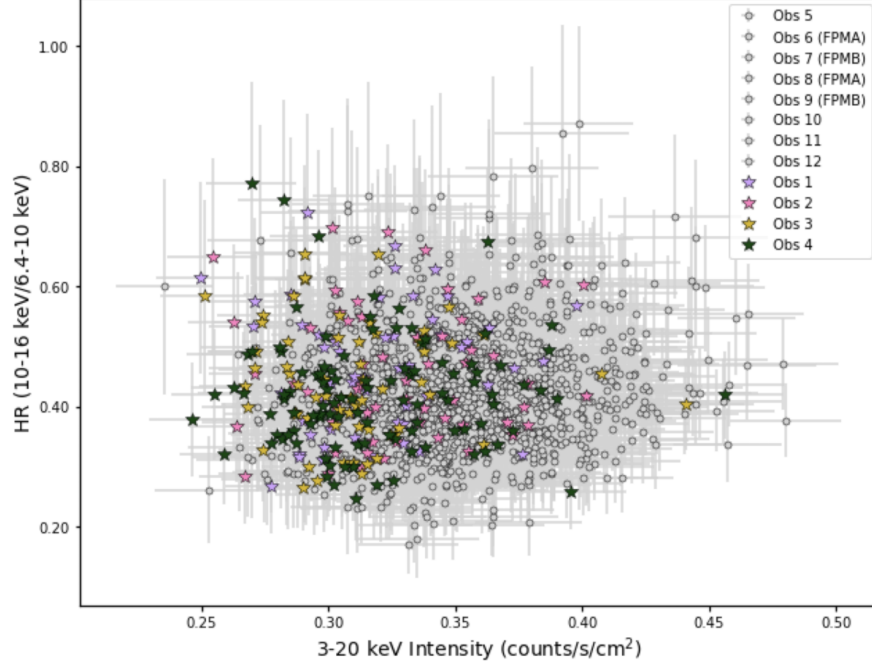


Figure 8: Composite HID highlighting the first four observations

Obs	Sequence ID	FPM	R_{in} (diskbb)	Banded R_{in} (bbody)	Luminosity
8	60002032002*	A	11.84 km		$2.90e+37$ erg/s
5	60002032004	A	18.40 km	16.84 km	$3.07e+37$ erg/s
7	60002032006	A	19.55 km	20.14 km	$2.93e+37$ erg/s
3	60002032008	A	17.91 km	19.58 km	$2.94e+37$ erg/s
1	90101008002	A	18.93 km	18.73 km	$3.53e+37$ ergs/s
		B	18.29 km	17.43 km	$3.34e+37$ erg/s
2	60402007002	A	16.04 km	17.53 km	$3.15e+37$ erg/s
4	60402007004	A	13.45 km	13.60 km	$3.08e+37$ erg/s
6	90101008004	A	17.93 km	15.41 km	$3.59e+37$ erg/s
		B	20.04 km	19.07 km	$3.66e+37$ erg/s
9	60002032010	B	17.41 km	17.11 km	$3.28e+37$ erg/s
10	60201020002	B	17.94 km	17.52 km	$3.39e+37$ erg/s

Figure 9: Highlighting calculated values of the first four observations

For further results, the link to all of the data I have tabulated on GX 9+9 are located in the Overleaf document [here](#).

5 References

- [1] Hansinger, G., & van der Klis, M. 1989, A&A, 225, 79
- [2] Ludlam, R. M., Miller, J. M., Barret, D., et al. 2019, ApJ, 873, 99
- [3] Harrison, F. A., Craig, W. W., Christensen, F. E., et al. 2013, ApJ, 770, 103
- [4] Grefenstette, B. W., Ludlam, R. M., Thompson, E. T., et al. 2021, ApJ, 909, 30
- [5] Madsen, K. K., Christensen, F. E., Craig, W. W., et al. 2017, J. Astron. Telesc. Instrum. Syst. 3(4), 044003
- [6] Savolainen, P., Hannikainen, D. C., Vilhu, O., et al. 2009, Mon. Not. R. Astron. Soc. 393(2), 596-578